

Active knee joint exoskeleton for stair ascent augmentation

Zongwei ZHANG, Jizhuang FAN*, Hongzhe JIN*, Tianjiao ZHENG, Sikai ZHAO, Shun MA, Jie ZHAO & Yanhe ZHU*

State Key Laboratory of Robotics and Systems, Harbin 150080, China

Received 27 August 2018/Revised 3 December 2018/Accepted 8 January 2019/Published online 14 April 2020

Citation Zhang Z W, Fan J Z, Jin H Z, et al. Active knee joint exoskeleton for stair ascent augmentation. *Sci China Inf Sci*, 2021, 64(3): 139204, <https://doi.org/10.1007/s11432-018-9767-6>

Dear editor,

Stair climbing is a strenuous daily movement that is challenging for older adults and those with lower limb weakness. In this study, we describe a novel stairclimbing exoskeleton that was designed to help weak-kneed people to climb stairs and help workers to carry heavy loads up stairs (Figure 1(a)). The exoskeleton has a hybrid control method that enables different performances in the stance phase and the swing phase. A switching controller guarantees the stability of the transition. Evaluations have showed that the exoskeleton can produce the torque required for stairclimbing.

Level ground walking and stairclimbing need different driving powers and joint motion ranges in both the sagittal and frontal planes [1]. During level ground walking, the knee joint acts as a passive joint, while the hip and ankle joints provide the driving forces [2]. In contrast, the motions during stairclimbing are mainly driven by the hip and knee joints in the frontal and sagittal planes, respectively [3]. Research on kinetics shows that stairclimbing requires more torque in the knee joint than that required during level ground walking, and that the torque of the knee joint is much larger than that of the other joints [4]. During stairclimbing, the knee joint provides more power and assistance than the hip joint. Thus, we considered that a powered knee joint exoskeleton would aid in stairclimbing.

Mechanical design. The robotic knee was designed as an active joint that helps the exoskeleton robot lift and support the human body in the stair ascent process. The knee joint reportedly requires a large amount of driving torque [3, 5]. Thus, if a motor and speed reducer system had been adopted directly, the mass and size of the driving system would have been unacceptably large, and so a new approach was needed to achieve this driving torque. We developed a linkage topology mechanism to overcome the contradiction between mass and driving torque [6]. The mechanical structure is illustrated in Figure 1(b). The rotational motion of the motor can be converted to the linear motion of the nut-slider through the ball screw, and the rotational movement of the

shank can be transferred from the crank mechanism. A shell (30 mm thick and 60 mm wide) has been created to contain the motor, crank mechanism, and other auxiliary devices. The leg, including the knee joint and the thigh, had a total weight of 2.9 kg, and the driving torque could be as large as 180 Nm.

The knee joint needs distinct angular displacements and torque in the stair ascent process compared with level ground walking [1, 3]. After the foot strikes the stairs, the joint moment increases considerably to support the body, while the joint displacement decreases to unbend the standing leg [4]. The simulation results of the torque and angular displacement of the joint showed that the proposed linkage knee joint supplied its largest moment at about 95° (Figure 1(c)), and thus met the requirements of stairclimbing [3].

Hybrid control of the robot. The exoskeleton robot applied a hybrid controller to fulfill the varying demands in different walking states. Different control strategies were used in the two phases (stance and swinging) and during transition between phases. The walking phase was identified by embedded contact sensors installed in the shoes. Each leg of the exoskeleton was treated as a serial robot. The kinetic equation of the leg was

$$H(\theta)\ddot{\theta} + C(\theta, \dot{\theta})\dot{\theta} + F(\theta)\dot{\theta} + G(\theta) = T_a + T_w, \quad (1)$$

where θ was a vector of the joint displacements. $H(\theta)$, $C(\theta, \dot{\theta})$, $F(\theta)$ and $G(\theta)$ were matrices of the inertia, Coriolis force, friction, and gravity force, respectively. T_a was the torque of the actuator, and T_w was the torque from the pilot.

- **Stance phase.** A gravity compensation controller was applied in the stance phase. The standing model of the exoskeleton was represented by an inverted pendulum model that regarded the connection between the center of mass and the supporting foot of the robot as an inverted pendulum (Figure 1(d)). It was assumed that the connecting bar was stretchable and had no mass, and the driving force F_g was treated as the generalized knee torque. It was also assumed

* Corresponding author (email: fanjizhuang@hit.edu.cn, hongzhejin@hit.edu.cn, yhzhu@hit.edu.cn)

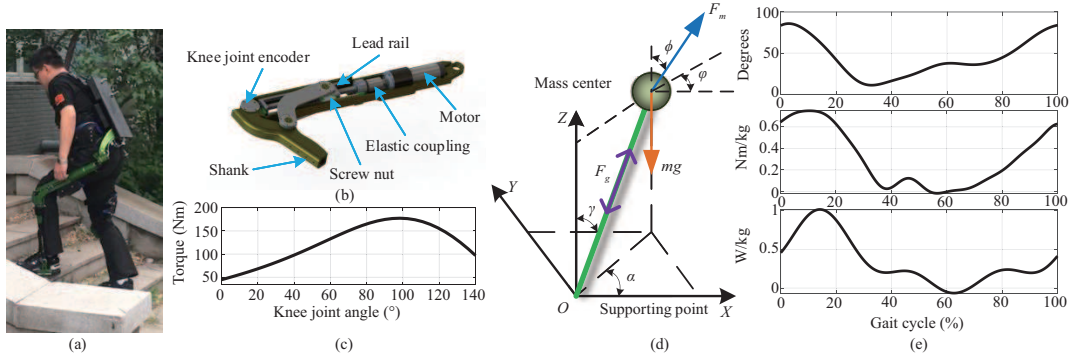


Figure 1 (Color online) (a) The proposed novel lower extremity exoskeleton with an active knee joint for stair ascent augmentation; (b) mechanical design of the knee joint; (c) moment analysis of the linkage knee joint; (d) inverted pendulum model in the stance phase; (e) evaluation of the exoskeleton during stair climbing.

that the human-machine interaction force F_m was a concentrated force applied on the simplified center of mass. The kinetic equation of the stance phase was

$$m \begin{bmatrix} \ddot{x} \\ \ddot{y} \\ \ddot{z} \end{bmatrix} = \begin{bmatrix} S_\gamma C_\alpha & S_\phi C_\varphi & 0 \\ S_\gamma S_\alpha & S_\phi S_\varphi & 0 \\ C_\gamma & C_\phi & 1 \end{bmatrix} \begin{bmatrix} F_g \\ F_m \\ -mg \end{bmatrix}, \quad (2)$$

where $S_\gamma = \sin \gamma$, $C_\gamma = \cos \gamma$, $S_\phi = \sin \phi$, $C_\phi = \cos \phi$, $S_\alpha = \sin \alpha$, $C_\alpha = \cos \alpha$, m was the mass of the simplified inverted pendulum model, g was the acceleration of gravity, and α , γ , ϕ , φ were the angles shown in Figure 1(d). To help the wearer support the body or carry loads, the exoskeleton robot provided a supporting force in the direction of gravity, while the wearer only provided small forces to maintain balance and drive the exoskeleton. Thus, the control equation was expressed as

$$F_g \cos \gamma = mg. \quad (3)$$

The wearer's trajectory in the joint space was defined as θ_r . Define $\Delta\theta = \theta_r - \theta$, $\Delta\dot{\theta} = -\dot{\theta}$ and $\Delta\ddot{\theta} = -\ddot{\theta}$. The wearer's torque was defined as $T_w = K_{ep}\Delta\theta + K_{ed}\Delta\dot{\theta}$, where K_{ep} and K_{ed} were positive definite matrices. Thus, the kinetic equation of the stance phase was

$$H\Delta\ddot{\theta} + (C + K_{ed})\Delta\dot{\theta} + K_{ep}\Delta\theta + \Delta F + \Delta G = 0, \quad (4)$$

where $\Delta F = (F(\theta) - \hat{F}(\theta))\dot{\theta}$ and $\Delta G = G(\theta) - \hat{G}(\theta)$, and $\hat{F}(\theta)$ and $\hat{G}(\theta)$ were the estimated values of $F(\theta)$ and $G(\theta)$, respectively. In the following parts, we have assumed that $\Delta F = 0$ and $\Delta G = 0$.

• **Swing phase.** A zero-force following controller was used to track the motions of the swing leg. Force sensors were installed on the linkage structure to detect the interactive forces between the robot and human. The control law was defined as

$$T_a = \tau - K_D\dot{\theta} + \hat{F}(\theta)\dot{\theta} + \hat{G}(\theta), \quad (5)$$

where τ was determined as $\tau = K_p f - K_d \dot{f}$, $f = K_{sp}\Delta\theta$ were forces from the force sensors in the joint space, and K_p , K_d , K_D , K_{sp} were positive definite matrices. Substituting (5) into (1) yields the kinetic equation of the swing phase as

$$H\Delta\ddot{\theta} + K_{dw}\Delta\dot{\theta} + K_{pw}\Delta\theta + \Delta F + \Delta G = 0, \quad (6)$$

where $K_{dw} = C + K_D + K_{ed} - K_d K_{sp}$ and $K_{pw} = K_{ep} + K_p K_{sp}$.

• **Switching controller.** To guarantee the stability of the hybrid control method, a switching controller was proposed [7]. The state variable was defined as $X = [\Delta\theta, \Delta\dot{\theta}]$. Define the time set σ as

$$\sigma = \{t | t = t_s + k_1 T_1\} \cup \{t | t = t_s + k_1 T_1 + k_2 T_2\}, \quad (7)$$

where $s, k_1, k_2 \in \mathbb{Z}_+$, t_s was the start time, and T_1 and T_2 were the base periods in the stance phase and the swing phase, respectively. The hybrid control law was defined as

$$\dot{X} = \phi(t)A_{st}X + (1 - \phi(t))A_{sw}X, \quad (8)$$

where A_{st} and A_{sw} were the state matrices of the stance phase and the swing phase, respectively. From (4) and (6),

$$A_{st} = \begin{bmatrix} 0 & I \\ -H^{-1}K_{ed} & -H^{-1}(C + K_{ed}) \end{bmatrix}, \quad (9)$$

$$A_{sw} = \begin{bmatrix} 0 & I \\ -H^{-1}K_{pw} & -H^{-1}K_{dw} \end{bmatrix}, \quad (10)$$

where I is the identity matrix. Define $\phi(t)$ as

$$\phi(t) = \begin{cases} 1, & t \in (t_s, t_s + k_1 T_1), \\ 0, & t \in (t_s + k_1 T_1, t_{s+1}), \end{cases} \quad (11)$$

where $t_{s+1} = t_s + k_1 T_1 + k_2 T_2$. At the instant when $t = t_s + k_1 T_1$, the controller switches from the stance to the swing phase. To enable the wearer to feel little impulsive force, the exoskeleton must ensure that the control torque is smooth. Furthermore, at the instant when $t = t_{s+1}$, the system switches from the swing phase to the stance phase; thus, to enable the exoskeleton to support a greater amount of load, the exoskeleton had to keep its states continuous. Then, we get

$$X^+(t_s + k_1 T_1) = S_{wt}X^-(t_s + k_1 T_1), \quad (12)$$

$$X^+(t_{s+1}) = S_{tw}X^-(t_{s+1}), \quad (13)$$

where S_{wt} and S_{tw} were the switching matrices from the stance to the swing phase and from the swing to the stance phase, respectively. Knowing the state at $t = t_s$, we calculated the following states at the switching times as

$$\begin{aligned} X(t_s + k_1 T_1) &= S_{wt}e^{(A_{st}k_1 T_1)}X(t_s), \\ X(t_{s+1}) &= S_{tw}e^{(A_{sw}k_2 T_2)}X(t_s + k_1 T_1). \end{aligned} \quad (14)$$

Define $A_{\text{dist}} = S_{\text{tw}}e^{(A_{\text{sw}}k_2T_2)}S_{\text{wt}}e^{(A_{\text{st}}k_1T_1)}$, and then

$$X(t_{s+1}) = A_{\text{dist}}X(t_s). \quad (15)$$

From the discrete linear Lyapunov theorem, for a positive definite matrix P , there exists a $V(x)$:

$$V(X(t_s)) = X^T(t_s)PX(t_s). \quad (16)$$

For $\forall \varepsilon \in [0, k_1T_1] \cup [0, k_2T_2]$, define $M = \max\{\|e^{A_{\text{st}}\varepsilon}\|^2, \|S_{\text{tw}}e^{A_{\text{sw}}\varepsilon}S_{\text{wt}}e^{A_{\text{st}}k_1T_1}\|^2\}$; thus for $\forall t \geq t_s$, we have

$$V(X(t)) \leq MV(X(t_s)), \quad (17)$$

$$\Delta V = X^T(t_s)(A_{\text{dist}}^T P A_{\text{dist}} - P)X(t_s), \quad (18)$$

where $\Delta V = V(X(t)) - V(X(t_s))$. If all the eigenvalues of A_{dist} lay within the open unit disc about the origin, $V(x)$ is decreasing and bounded, which means that the hybrid controller is asymptotically stable.

Evaluation. The effectiveness of the proposed exoskeleton and performance of the hybrid controller were evaluated with a subject wearing the proposed prototype robot while ascending stairs with a 30-kg load. The mean movement angle, moment, and driving power of the active knee joint are shown in Figure 1(e). The supporting foot left the stairs at about 45% of the walking gait, after the joint angular displacement had decreased to unbend the standing leg. The moment of the joint initially increased and then decreased gradually to support the standing leg. The trend of the power reflected this phenomenon, and the larger exported moment from the pilot led to negative power in the swing phase. During the stair ascent process, the knee can reportedly bend up to 75° , and the moment of the knee joint

can reach 1 Nm/kg [3]. In our experiments, the maximum bending angle of the knee joint was 85° and the maximum moment was 0.8 Nm/kg. This suggests that the proposed exoskeleton could compensate for about 80% of the largest torque needed during stair ascent movement with a load of 30 kg.

Acknowledgements This work was supported by National Key R&D Program of China (Grant Nos. 2018YFB1305400, 2017YFB1302301) and Joint Research Fund (Grant No. U1713201) of NSFC and Shenzhen.

References

- 1 Novak A C, Brouwer B. Sagittal and frontal lower limb joint moments during stair ascent and descent in young and older adults. *Gait Posture*, 2011, 33: 54–60
- 2 Asbeck A T, de Rossi S M M, Holt K G, et al. A biologically inspired soft exosuit for walking assistance. *Int J Robot Res*, 2015, 34: 744–762
- 3 Nadeau S, Mc Fadyen B J, Malouin F. Frontal and sagittal plane analyses of the stair climbing task in healthy adults aged over 40 years: what are the challenges compared to level walking? *Clinical Biomech*, 2003, 18: 950–959
- 4 Winter D A. Energy generation and absorption at the ankle and knee during fast, natural, and slow cadences. *Clinical Orthop Related Res*, 1983, 175: 147–154
- 5 Mc Fadyen B J, Winter D A. An integrated biomechanical analysis of normal stair ascent and descent. *J Biomech*, 1988, 21: 733–744
- 6 Zhang Z W, Zhu Y H, Zheng T J, et al. Lower extremity exoskeleton for stair climbing augmentation. In: *Proceedings of International Conference on Advanced Robotics and Mechatronics*, Singapore, 2018. 762–768
- 7 Das T, Mukherjee R. Shared-sensing and control using reversible transducers. *IEEE Trans Control Syst Technol*, 2009, 17: 242–248